Chapter 19

# Using Raman Spectroscopy for Characterization of Aqueous Media and Quantification of Species in Aqueous Solution

Ivana Durickovic

Additional information is available at the end of the chapter

http://dx.doi.org/10.5772/64550

**Abstract**

In this chapter, the use of Raman spectroscopy (RS) for studies of aqueous solutions is shown. This technique is mainly used for the characterization of solid samples, but presents numerous features permitting its use for the analysis of aqueous media. Indeed, it possesses all the advantages of optical methods (versatility, rapidity, contact-less non-destructive measurement, etc.), but also offers possibilities for *in situ* measurements. The Raman spectrum will be influenced by several parameters such as the solution concentration or its temperature-phase. Thus, the analysis of a set of aqueous solutions of different concentrations in a certain temperature range can permit the identification of the specific effect of salt and temperature. A proper analysis based on the follow-up of the specific peak areas or intensities can permit the determination of the salt concentration or the phase transition of the studied solution. The analysis can be focused on the salt direct effect on the spectrum, analysis of the salt signature itself, or on its indirect effect on the water signature. The method for the characterization of aqueous solutions of some salts is presented: elaboration of calibration curves and concentration determination. As an application example, a special attention is devoted to aqueous solutions that are used in the winter maintenance domain (solution of acetates, formates, or chlorides), which are very relevant examples of aqueous solution behavior. A specific analysis set to determine the solution solid-liquid phase transitions is presented as well as the thus-constructed phase diagram.

**Keywords:** aqueous solutions, Raman spectroscopy, characterization, quantification, phase transition

## 1. Introduction

In this chapter, the possibility of using Raman spectroscopy (RS) for studies of aqueous solutions is shown. Section 2 is devoted to the description of the general principle and characteristics of Raman spectroscopy (RS) as a technique for the investigation of molecular structure. Since Raman spectra contain information not only on intra-molecular vibrations but also on vibrations of the crystal lattice and other solid movements, RS is a well-established technique for the studies on solid materials [1].

The aim of this chapter is to show the possibility of its use to study aqueous solutions and chemical species dissolved in water. The application of RS on the study of aqueous media is more complicated than in solids, but is still very efficient if a proper signal treatment is applied. In order to show the different possibilities of RS for the characterization of water media, a special attention is devoted to one application example: aqueous solutions that are used in the winter maintenance domain (solution of acetates, formates, or chlorides). The possibility of its use for the detection of some water pollutants is also discussed.

In the case of water quality, there is a need for a device presenting a high polyvalence degree to detect and to quantify several chemical species in aqueous solutions but also to discriminate them from each other. There is an increasing need for a technique that could permit *in situ* measurements and continuous monitoring of water.

However, the techniques actually used for the detection and quantification of chemicals in water often do not respond to these criteria [2]. Some techniques, such as the widely used solution conductometry, are fully dedicated to one chemical species or are not able to make an accurate discrimination between different chemical species. In other cases, the quantification of chemicals in water media usually needs the combination of several techniques such as ionic chromatograph and electrical conductivity. This approach is then not appropriate for *in situ* measurements and are time consuming, inducing a time delay between the sample collection and analysis. The same remark concerns the inductively coupled plasma atomic emission spectroscopy, which permits to detect chemical atoms.

On the other hand, previous studies indicated the great potential of the optical and spectroscopic tools in the detection of salts in solutions and, more specifically, RS, which could then permit to avoid the inconveniences of the techniques mentioned above [3]. Indeed, as it is shown, RS can permit us to determine the nature and the quantity of chemical species present in water media, offering the possibility to discriminate the different species present. In addition, the RS is an all-optical method, so it possesses all the advantages of optical methods (versatility, rapidity, contactless non-destructive measurement, etc.), as it will be detailed further on. Moreover, RS is generally more versatile and easier to set up *in situ*.

## 2. General principle of Raman spectroscopy

RS provides numerous information about the structure and chemical composition of the sample, information obtained by an illumination of the sample with a monochromatic

http://dx.doi.org/10.5772/64550

radiation (laser beam) that excites the vibrational structure of molecules; RS is thus called a vibrational spectroscopy. As illustrated in **Figure 1**, the radiation coming to the sample undergoes two types of scattering: Rayleigh scattering, where the radiation is at the exact same frequency as the excitation laser line (**υ**), and Raman scattering where the scattered radiation has a different frequency (**υ'**). The difference between the two frequencies, called "Raman shift" (**Δυ**), is the consequence of the interaction of the radiation with the sample molecules by the means of the vibrations of the chemical bonds present in the sample [4–6]. Note that, because it is a difference value, the Raman shift is consequently totally independent of the frequency of the incident radiation.

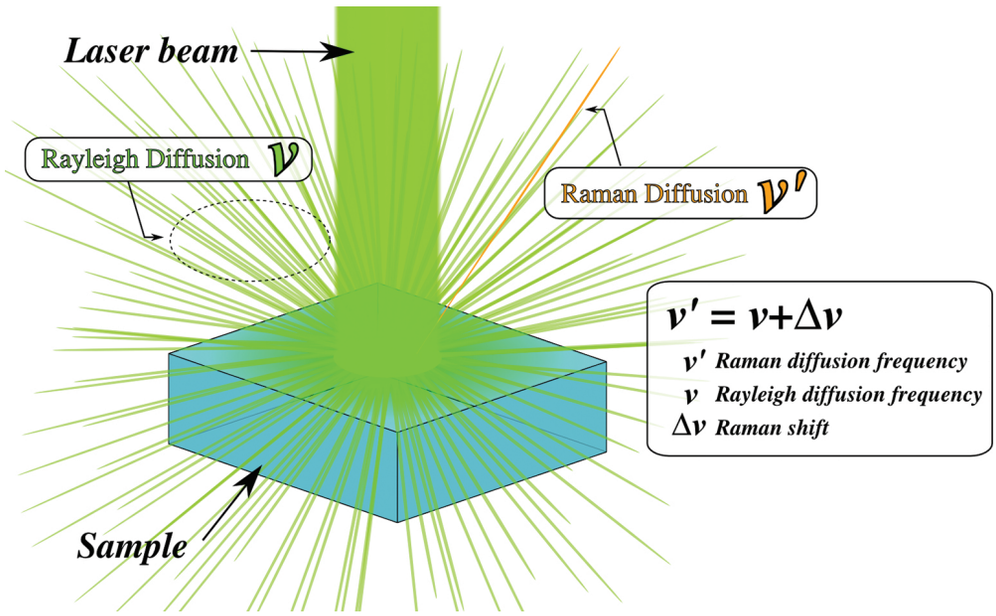


**Figure 1.** Schematic representation of the Rayleigh and the Raman diffusions.

In order to properly extract the Raman shift, the radiation coming from the Rayleigh diffraction has to be filtered out with a notch or a band pass filter from the total radiation before being collected on the spectrometer sensor (generally a CCD). Thus, only the radiation with a different wavelength than the incident laser beam is analyzed.

### 2.1. Raman spectrum

The results of the measurements are depicted graphically as Raman spectra. The intensity of the scattered light is plotted for each energy (frequency) of light. The frequency axis represents the Raman shift **Δυ**, as it is the shift in energy/frequency of the light that is of particular interest. In vibrational spectroscopy, the frequency is traditionally measured in a unit called the "wavenumber" (number of waves per cm, $cm^{-1}$), which is directly proportional to energy. Wavenumbers are easily converted into the more familiar wavelength scale by calculating the reciprocal.

A thus-plotted Raman spectrum is composed of peaks, where each peak corresponds to a specific vibration of a chemical bond present in the sample. The more complex the chemical composition, the richer is its Raman spectrum.

When the specific vibration is represented by a wider peak, we are generally talking about a "band" that can be composed of several peaks. In this case, each peak represents the vibration of the same chemical bond, but its surrounding environment is slightly different, provoking a frequency shift. Thus, the partly overlapping peaks form a resulting band that is covering a more or less large range of frequencies.

### 2.2. Information accessible

By the analysis of the different Raman peaks present, a Raman spectrum can give us numerous qualitative and quantitative information on the sample, as presented in **Figure 2**.

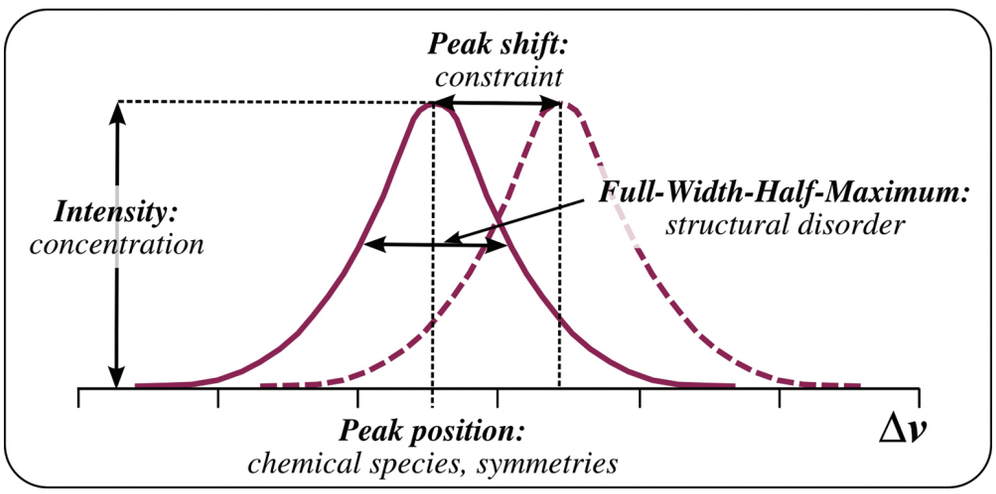


**Figure 2.** Information accessible from a Raman spectrum [6].

Three spectral parameters can be derived from the analysis of a Raman line.

The **position of the peak** defined by its maximum corresponds to the vibration frequency of the chemical species. Since each chemical bond has its own characteristic vibrations, the position of the peaks lead to the identification of the chemical species. The determination of the peak locations in a Raman spectrum is sensitive enough for the recognition and the specification of chemical species in heterogeneous samples [7].

The **peak intensity** is related to the corresponding chemical species concentration. In order to determine this parameter, it is necessary to use normalization of the integrated intensity of the Raman line as the peak intensity is also sensitive to the laser power. The follow-up of the relative changes in the integrated intensities of peaks is then necessary for excluding the laser influence and to determine correctly the species concentration.

Furthermore, the full width half maximum (FWHM) reflects the order character of the sample: structure with the lower the FWHM, the higher the local order.

http://dx.doi.org/10.5772/64550

Thereby, the peak position, the linewidth, and intensity extracted from a Raman line can be used for the determination of some physico-chemical parameters such as the sample phase or constraint [8]. The analysis of all the peaks present in the spectrum gives us an insight on the sample composition and structure. RS can thus be used to determine various quantities that can affect the vibrational state (modes/peaks) specific to a substance.

In addition, specific Raman peaks are sensitive not only to the above-mentioned composition or concentration of the substance under study but also to external parameters such as the temperature or the pressure that affect the structure of the sample. Thus, the spectroscopic follow-up of a sample can permit to identify which chemical bond is affected by a change of an external parameter and to identify the constraint through the resulting peak shift. This aspect is explained further in this chapter in Section 3.2.

Since a Raman spectrum gives details on the chemical composition, molecular structure, and molecular interactions, it is hence considered as a chemical compound fingerprint at a molecular or crystalline level.

### 2.3. Advantages

RS is useful for chemical analysis for several reasons [9, 10]. As many optical techniques, it is non-destructive and non-intrusive, permitting to perform contactless measurements. Furthermore, in contrast with most other chemical analysis techniques, it does not require any specific sample preparation. Moreover, this technique requires a small volume of the substance, in the order of 1 $\mu m^3$, for the analysis and it is possible to use optical fibers for deported measurement. This kind of set up is particularly well adapted for *on-site* measurements (on the field or in an industrial context). Furthermore, as a Raman spectrum can be acquired in the range of time of seconds, RS permits an almost "real-time" monitoring of chemical reactions. Depending on the experimental set up and on the application aimed, it can offer different spatial resolutions (from 1 μm to 1 cm). An additional advantage of RS is the possibility to analyze samples in solid, liquid, or gaseous state.

It is to note that RS offers the possibility to use lasers in a large spectral domain, going from the ultraviolet to the near infrared (IR). The choice of the most appropriate laser to use will depend on the nature of the sample under study. Indeed, the absorption, the fluorescence, the solidity toward light exposure, and more generally the interaction between light and the sample have to be taken into account. For the specific case of aqueous solutions, the most appropriate laser is in the visible green light (514 or 532 nm), which permits to diminish the fluorescence.[1] Furthermore, the excitation wavelength will have an important impact on experimental capacities; the laser wavelength $\lambda$ will influence Raman intensity, proportional to $\lambda^{-4}$, and spatial resolution, defined by a diameter equal to $1.22\,\lambda / NA$, the numerical aperture of the objective used.

1 In fluorescence, the incident excitation light is completely absorbed, transferring the system to an excited state and producing a photon with a different frequency. The fluorescence photons, which are of lower energy, are emitted after a certain resonance lifetime.

RS presents also some inconveniences and limits, but the technology development offers possibilities to overcome most of them. For instance, Raman signal of some compounds can be weak comparing to the total signal, making it difficult to determine small concentrations. A stronger signal can obviously be obtained by the increase of the laser power, but the influence of the laser on the sample state could be strong enough to be problematic for the analysis or even induce a sample damage. To compensate this detrimental effect, the recent technological development improved significantly the performance of multichannel detectors, leading to a considerable increase of the sensitivity of Raman spectrometers.

Another limiting factor is the fluorescence, which can be much higher than the Raman signal, dominating in intensity the Raman effect, at times diluting it completely in the signal noise. However, as the Raman effect is independent on the excitation frequency, it is often possible to overcome this difficulty by choosing an appropriate laser.

Despite these few restrictions, RS appears well adapted for the analysis of aqueous solutions. Compared to infrared spectroscopy where the spectrum of water is so strong and complex that it interferes with the signatures of chemical species, the Raman spectrum is not sensitive to aqueous absorption bands that are weak and unobtrusive. The analysis of liquids is easier, thanks to the transparency of glass containers in the spectral domains concerned.

## 3. Spectroscopic analysis of water

### 3.1. Specific water signature

The structure of water has been studied for decades by both infrared (IR) and RS [11–15]. The normal modes of water are nowadays well known and detailed on **Figure 3**; The spectral band corresponding to the O—H bending (noted $v_2$) is located at about 1600 $cm^{-1}$, and to the O—H stretching band around 2900–3700 $cm^{-1}$. This broad range of the Raman spectrum of liquid water is composed of symmetric (noted $v_1$) and asymmetric (noted $v_3$) O—H stretching vibrations [14, 16, 17].

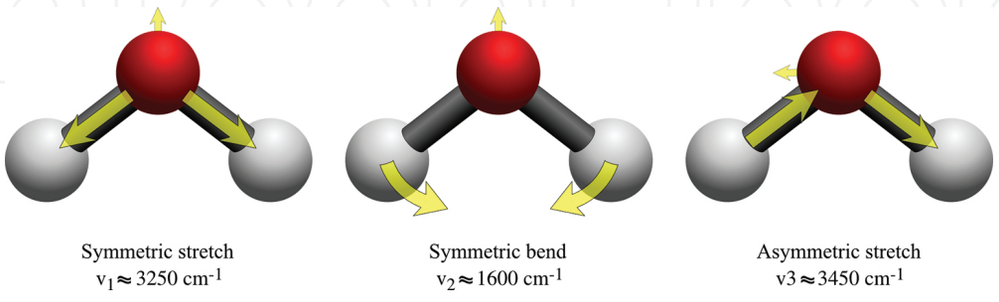


**Figure 3.** Normal modes of water.

In the literature, a special attention is devoted to the study of the O—H stretching region [18, 19]. The particular interest for this region originates from the fact that it is generally considered

http://dx.doi.org/10.5772/64550

to be closely related to the structure of water [20, 21] because it is an indicator of the hydrogen-bonding network [22, 23]. Moreover, even though it is well known that this band constitutes of the symmetric and asymmetric O—H stretching, further designations of these normal modes are still not well elucidated. It is generally admitted that all the bands of water are made up from contributions from different components from water molecules in different hydrogen bonded environments. In order to analyze this region in a more detailed way, it is necessary to proceed to a deconvolution of the band corresponding to this complex contribution of the water spectrum into various peak components, to assign each vibrational mode and to get back to their molecular origins. However, when it comes to bands that are as large as the O—H stretching band, the decomposition is rather complicated and numerous deconvolution models can be found in the literature. Depending on the authors, different number of components as well as different mechanisms involved are considered. The use of two to five components for deconvolution is suggested to correctly describe the O—H stretching band [18, 24–27]. The most commonly proposed deconvolution contains five components [28–30]. An example of such a deconvolution of the O—H stretching band is presented in **Figure 4**.

It is to note that even when using the same number of components for the deconvolution, different results can be found and different attributions proposed. For each deconvolution, different hydrogen bond properties, such as their number, angle or length, are used to define the attributions [18, 27, 30–33]. Generally speaking, lower frequency components are attributed to water molecules with stronger hydrogen bonds and higher frequency components have weaker hydrogen bonds [34].

All these studies show that, besides the intra-molecular O—H pairs, intermolecular O—H linked by hydrogen bonds contribute to the O—H stretching. The role of the hydrogen bonds is therefore of great importance for the understanding of this spectral range. This bond being

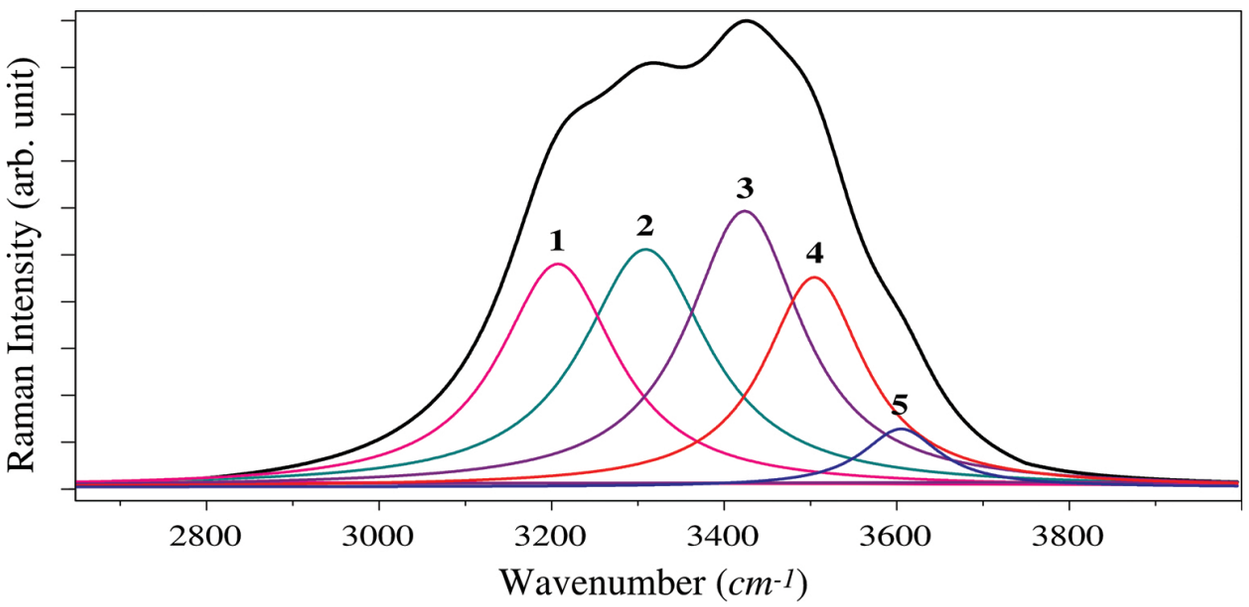


**Figure 4.** Example of deconvolution of the O—H stretching band into five sub-bands [28].

flexible is sensitive to temperature [35] and the presence of ions. The study of this spectral region can therefore be used for the determination of the water phase or for the detection of ions dissolved in water, as it will be presented thereafter.

### 3.2. Phase effect

As a molecule, water can be present at three different phases—solid, liquid, and gaseous—the state depending on the environmental conditions, namely the pressure and the temperature. This chapter concentrates on the solid-liquid phase transition, with a special focus on measurements performed on atmospheric pressure, the application example being the winter maintenance domain.

As mentioned earlier, the O—H stretching band is considered to be closely related to the structure of water. It is expected that the morphology of this band will be modified by a change in the temperature or in its chemical composition, as it can be seen on **Figure 5** where normalized spectra of liquid water and ice are compared.

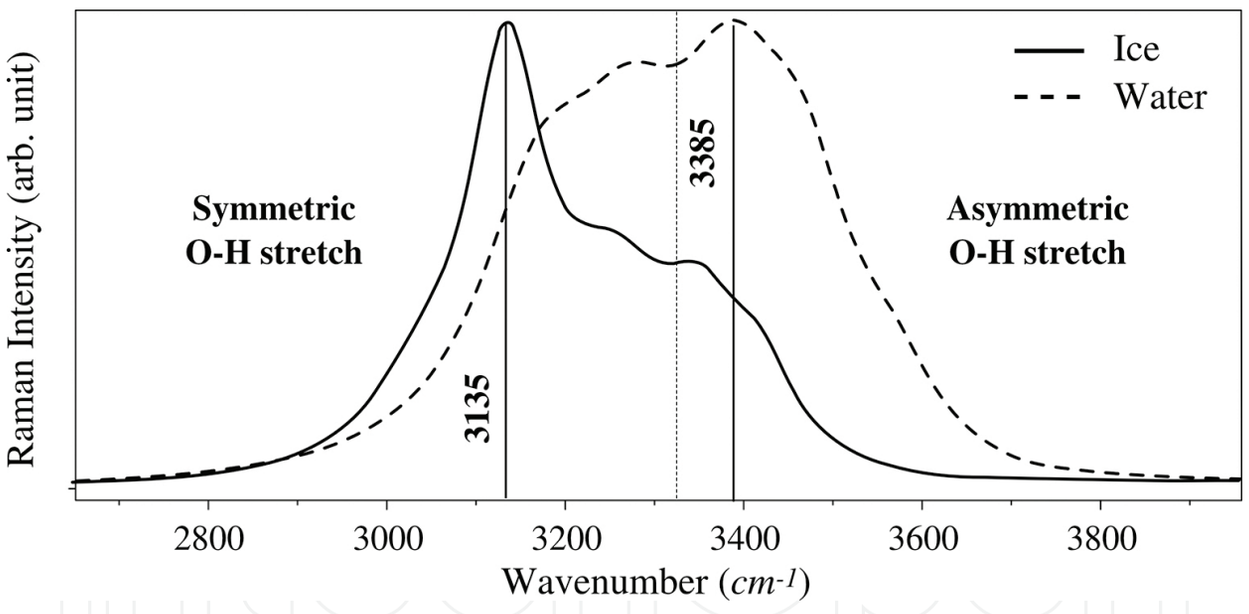


**Figure 5.** Raman signature of the O—H stretching region for water in its liquid (at 20°C) and solid form (at −20°C) obtained with a 532-nm laser beam at 100 mW.

In the case of liquid water, molecules are in constant movement, provoking continuous creation and break of hydrogen bonds that are rather weak. Water can be considered as a mixture of isolated water molecules and water molecules forming clusters by the hydrogen bonds [14]. Hence, all contributions, in terms of number of hydrogen bonds present, contribute to the O—H stretching band. This leads to a broad spectrum with the symmetric and asymmetric regions of the band that are almost equally represented. An average number of hydrogen bonding for

http://dx.doi.org/10.5772/64550

each molecule is found to be 2.75 [29], which is manifested by a slightly greater intensity at 3385 $cm^{-1}$ corresponding to the contribution possessing three H-bonds.

In the case of ice, on the other hand, the decrease of temperature will strengthen the hydrogen bonds, leading to weaker O—H bonds, which will thus vibrate at lower frequencies. Furthermore, besides the shift toward the lower frequencies, due to the increased importance of intermolecular hydrogen bonding at lower temperature, the lower part of the spectrum, related to fully H-bonded atoms, enhances and becomes narrower [36].

### 3.3. Phase transition determination

Since the spectra of liquid water and ice are significantly different, the combination of Raman spectrometry and micro-thermometry can lead to precise detection of the water phase transition. Spectra obtained in the −3 to 3°C temperature region were collected and their O—H stretching band presented in **Figure 6**. It is reminded that the study is focused on the O—H stretching band, as it is the spectral region considered to be closely related to the structure of water and which is thus expected to be the most influenced by a change of temperature.

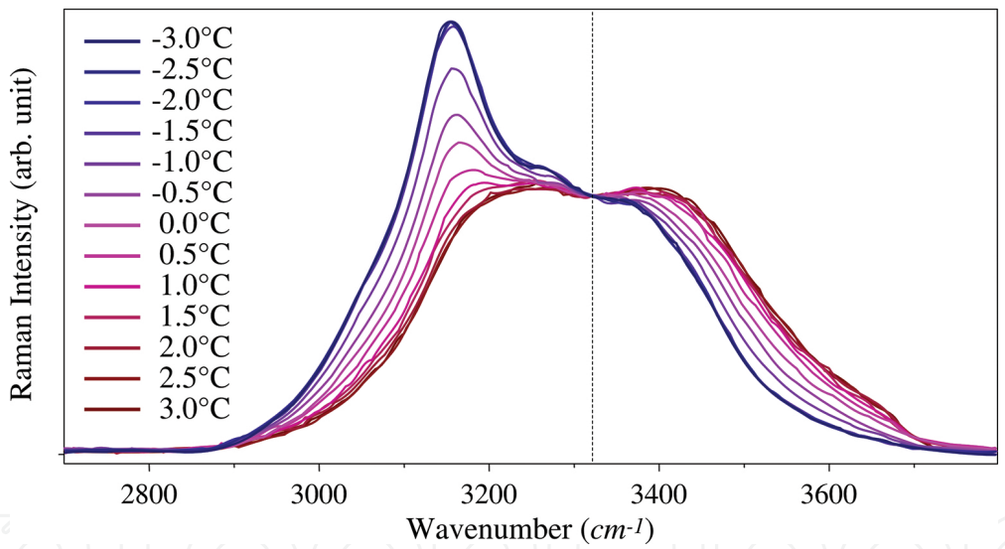


**Figure 6.** Raman spectra of water between −3 and 3°C, obtained with a 532-nm laser beam at 100 mW.

The center of the O—H stretching bond is located around 3325 $cm^{-1}$. The temperature modification induces large changes in the shape and the intensity of the O—H stretching region in both the part corresponding to symmetric and asymmetric stretching vibrations. It can be considered that the lower frequency part of the spectrum (between 2900 and 3325 $cm^{-1}$) roughly corresponds to the ordered solid phase as this contribution is related to fully H-bonded atoms, whereas partly H-bonded and free O—H are expressed in the upper frequency part, characteristic of the liquid phase [30]. It is then possible to follow the phase transition by the relative evolution of these two parts of the O—H stretching region as the evolution of the order/disorder of the water structure can be reflected from the values of their intensities. Thus, a spectral

marker $S_D$, can be defined as the ratio of the asymmetric and the symmetric part of the O—H band, parts centered on 3385 and 3135 $cm^{-1}$, respectively, in order to detect the phase transition.

A method for the determination of the phase transition based on that principled was developed and tested [37]. That study showed that, for the calculation of the spectral marker, it is possible to use intensities at the peak maximum or integrated intensities of raw spectra.[2] The comparison of curves obtained by the calculation of ratios of simple intensities of the two most intense parts (c) and of integrated intensities of more (a) or less broad (b) spectral areas around the peak maximum is shown in **Figure 7**.

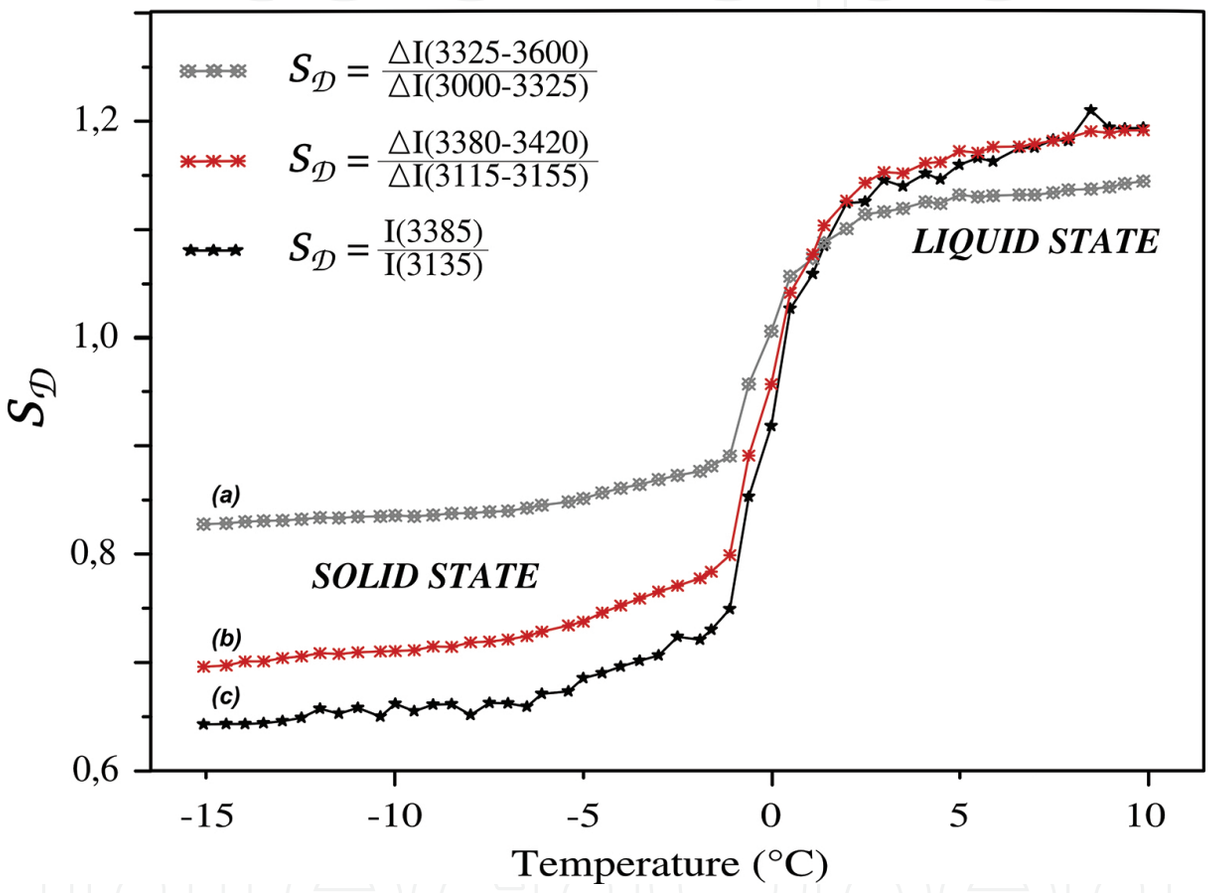


**Figure 7.** Plots of the spectral marker $S_D$ calculated with intensities (c) or integrated intensities (a, b) as a function of temperature [37].

The temperature of the phase transition is then determined by a simple calculation of the curve inflection point. The uncertainty of the phase temperature thus obtained is dependent on the speed of the temperature change during the measurements. In the case presented here, the speed was set to 0.5°C/minute, and the uncertainty obtained is about 0.5°C for each ratio tested (ratio of simple or integrated intensities).

2 The use of raw spectra permits to overcome the possible controversies about the deconvolution of the O—H stretching region. In this method, only two parts of the spectra that are affected by the temperature and phase change are then analyzed.

http://dx.doi.org/10.5772/64550

## 4. Spectroscopic analysis of aqueous media

A Raman spectrum of an aqueous solution will present specific the different O—H bond vibrations of water, as well as specific peaks of each chemical/salt diluted. Indeed, each type of salt (acetate, formate, nitrate, etc.) diluted in an aqueous solution presents specific signatures/peaks corresponding to the vibrations of the different chemical bonds constituting it. By the analysis of each peak, it is possible to identify the nature of the chemical present, as well as its concentration. Indeed, the systematic analysis of a set of aqueous solutions of different concentrations can permit the identification of the specific effect of the chemical. A proper analysis based on the follow-up of the specific peak intensities or areas can permit the determination of the chemical concentration. The analysis can be focused on the salt direct effect, on analysis of the salt signature, or on its indirect effect by the analysis of the water signature.

As presented earlier in this chapter, the peak intensity is linked to the concentration. Peak intensity measurements are thus used in most quantitative analyses. However, the absolute intensity of a Raman spectrum can vary considerably from one instrument to another as it is also sensitive to changes in instrumental resolution, calibration and signal/noise ratio, etc. Thereby, it is necessary to use integrated intensity, a measure of the total intensity of the band, which is much less sensitive to instrumental resolution [4].

### 4.1. Application to winter maintenance aqueous solutions

The application example will concern aqueous solutions used in winter maintenance where different anti-icing chemicals are spread on runways in order to maintain a proper grip.[3] This is a commonly employed technique to avoid the occurrence of ice or to generate its melting [38, 39]. The products used are mainly salts, heard as ionic compounds composed of cations and anions. Each of these salts contains an "active compound" permitting to lower the freezing temperature of the liquid present on the road surface [40]. The most commonly employed anti-icing product for road winter maintenance is the NaCl (in France, up to 99% of the cases). The active compounds of the products applied on the airport surfaces are mainly acetates and formates of sodium or potassium for corrosion reasons [41].

#### *4.1.1. Concentration determination*

For the quantification of the molecules of interest, the anti-icing active compounds, it is necessary to construct appropriate calibration curves. For that purpose, solutions with well known composition and concentration of each active compound are prepared and analyzed spectroscopically. The first step is to identify the spectral signature of an analyzed compound. Raman spectra of the different salts used in winter maintenance are presented on **Figure 8**. The more complex the chemical composition, the richer is its Raman spectrum;

3 The quantification of the active compound of these products is necessary for both the characterization of the nature of the commercial products and the optimization of the quantities applied on airport areas.

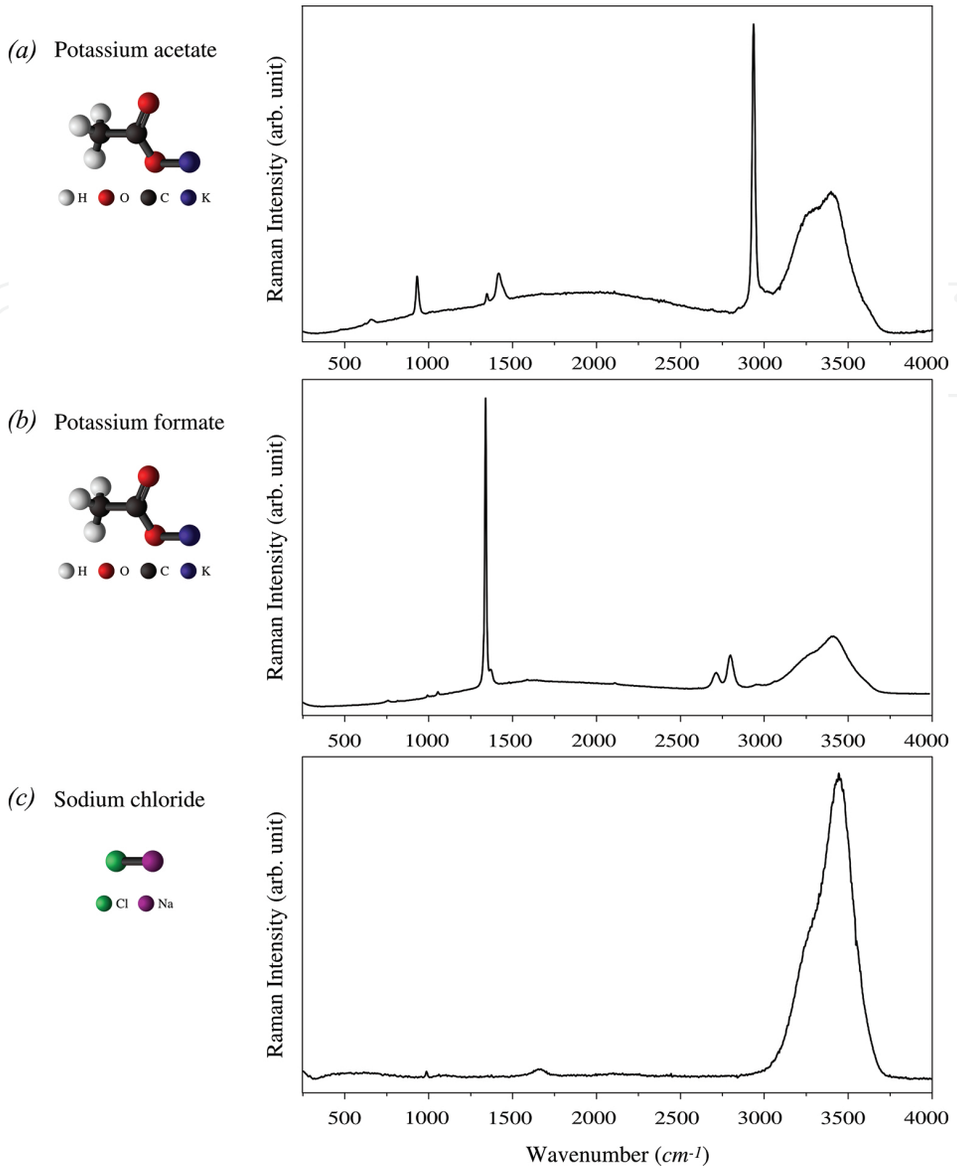


**Figure 8.** Raman spectra of aqueous solutions of the salts used in winter maintenance: potassium acetate (a), potassium formate (b), and sodium chloride (c) obtained with a 532-nm excitation wavelength.

The Raman spectrum of potassium acetate presents peaks corresponding to the vibrations of O—C—O bending, C—C stretching, $CH_3$ bending, C—O stretching and $CH_3$ stretching [42–45]. For potassium formate, the peaks corresponding to O—C—O and C—H bending, as well as C—O and C—H stretching [46–48] are present. The sodium chloride spectrum, on the other hand, presents only the peaks characteristic of the water, O—H bending and O—H stretching. Indeed, chemicals that present only monoatomic ions once dissolved in water (like NaCl gives [$Na^+$] and [$Cl^-$]), do not possess specific peaks, as they do not have bonds anymore [49, 50].

Clearly, it is not possible to use the same analysis method for the elaboration of the calibration curves for all these species. We then consider two cases: on the one hand, the case when the salt presents specific peaks, making it possible to detect its presence and concentration directly,

http://dx.doi.org/10.5772/64550

and, on the other hand, where the salt does not present any specific peak and it is only possible to detect and quantify it indirectly.

Furthermore, for a better baseline correction, it is possible to focus the study on only one part of the spectrum. In the case of winter maintenance salts presented below, the study considered the region above 2500 $cm^{-1}$.

#### *4.1.1.1. Direct concentration determination: $CH_3COOK$ and CHOOK*

For an optimized calibration curve, the analysis of aqueous solutions covering a large scale of concentrations is necessary. For the potassium acetate and formate, solutions with a weight percent up to 65 and 60%, respectively, were analyzed (**Figure 9**). The weight percent (wt%) is defined as the ratio of the mass of the salt dissolved $m_{salt}$ and the mass of the solution sample $m_{sample}$.

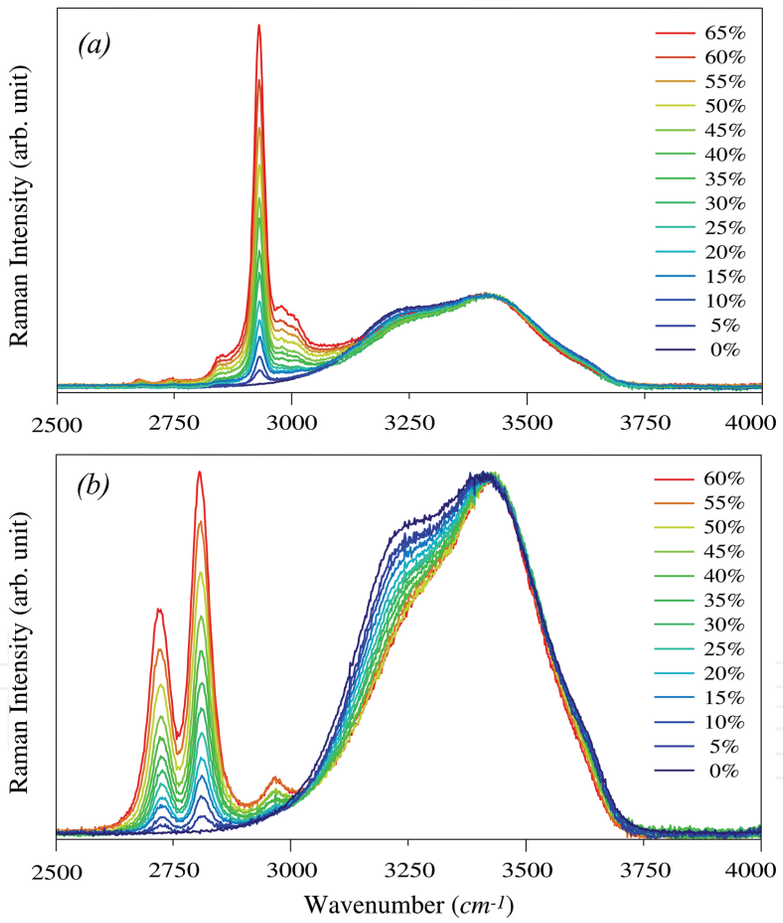


**Figure 9.** Normalized Raman spectra of aqueous solutions of potassium acetate (a) and potassium formate (b) with a weight percent between 0 and 65% and 0 and 60%, respectively. Spectra obtained with a 532-nm laser at 100 mW.

In **Figure 9** are presented spectra of potassium acetate and potassium formate solutions at different concentrations/weight percent in the 2500–4000 $cm^{-1}$ spectral region. This region contains, for both salts, a salt specific peak, as well as the O—H stretching band. As expected,

in both cases, the intensity of specific peaks increase with the concentration. A proper signal treatment permits to extract the effect of the active compound on the Raman spectra and to elaborate appropriate calibration curves. A calibration curve defines the relationship between an analytical signal produced by the analyte and its concentration.

In the simplest case, the calibration curve is linear and a simple linear regression permits to fit the analytical signal to the concentration. Most generally, however, the analysis is more complex since the calibration curves are often affected by overlapping bands, additional interfering components. The resultant calibration curves will often be non-linear [5].

On the whole, for the elaboration of a calibration curve, the calculation of the peak intensity as a function of the concentration can be used, however, it is important to ensure that the peak characteristics that will be calculated will be affected only by the compound itself. As mentioned before, in order to avoid the bias of spectral intensity caused by the experimental setup, it is recommended to use integrated intensity. Furthermore, experimental conditions, such as ambient light, can also influence the spectral intensity and even the integrated intensity. One way of overcoming all these difficulties and to maintain only the compound concentration influence is to use a ratio of integrated intensities [28].

Hence, for the elaboration of the calibration curves of potassium acetate and formate, a spectral marker $S_D$ is defined as a ratio of an integrated intensity of a specific peak $\Delta I_{salt}$, over the integrated intensity of the O—H asymmetric stretching vibrations $\Delta I_{OH}$. For the potassium acetate, the integrated intensity 2801–3001 $cm^{-1}$ including the $CH_3$ stretching band was chosen as $\Delta I_{salt}$, and for potassium acetate $\Delta I_{salt}$ was defined as the integrated intensity of the 2725–2809 $cm^{-1}$ region including the C—H symmetric stretch. For both cases, $\Delta I_{OH}$ was defined as the integrated intensity of the water 3324–3486 $cm^{-1}$ spectral region. The thus obtained calibration curves are presented in **Figure 10**.

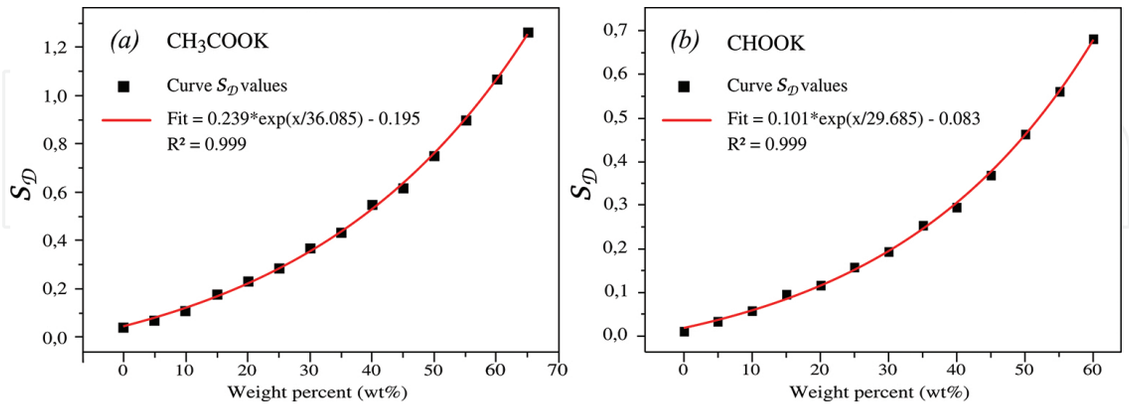


**Figure 10.** Calibration curves obtained for potassium acetate (a) and potassium formate (b). Both curves present an $R^2$ of 0.999.

In this particular case, there is a slight overlapping of the bands chosen, as there is a small contribution of the O—H band in the region of the C—H band. As a result, the resultant

http://dx.doi.org/10.5772/64550

calibrations curves obtained for the potassium acetate and potassium formate presents an exponential evolution.

These calibration curves can then permit not only to identify the presence but also to quantify these species in an aqueous solution. The precision of the method will depend on the quality of Raman spectra obtained. In general, with the 532 nm laser excitation and a 60 second accumulation time, it is possible to obtain a good signal/noise ratio permitting the quantification of these species with an 1% uncertainty. Depending on the application aimed, it is possible to diminish even more the uncertainty by analyzing more aqueous solutions in order to have more points for the calibration curves. For the winter maintenance application, however, the uncertainties aimed are rather high, 5%, and then this method is well-fitted just as it is shown here.

#### *4.1.1.2. Indirect concentration determination: NaCl*

The concentration determination by a direct analysis of a chemical specific peak is immediate and will, logically, offer better results. However, chemicals that dissolve in monoatomic ions do not possess specific peaks, as they do not have bonds [49, 50]. In order to detect their presence in water and to quantify them, it is necessary to analyze the water signature and deduce information on the chemical through their influence on the water structure. A typical example of this behavior is sodium chloride, NaCl.

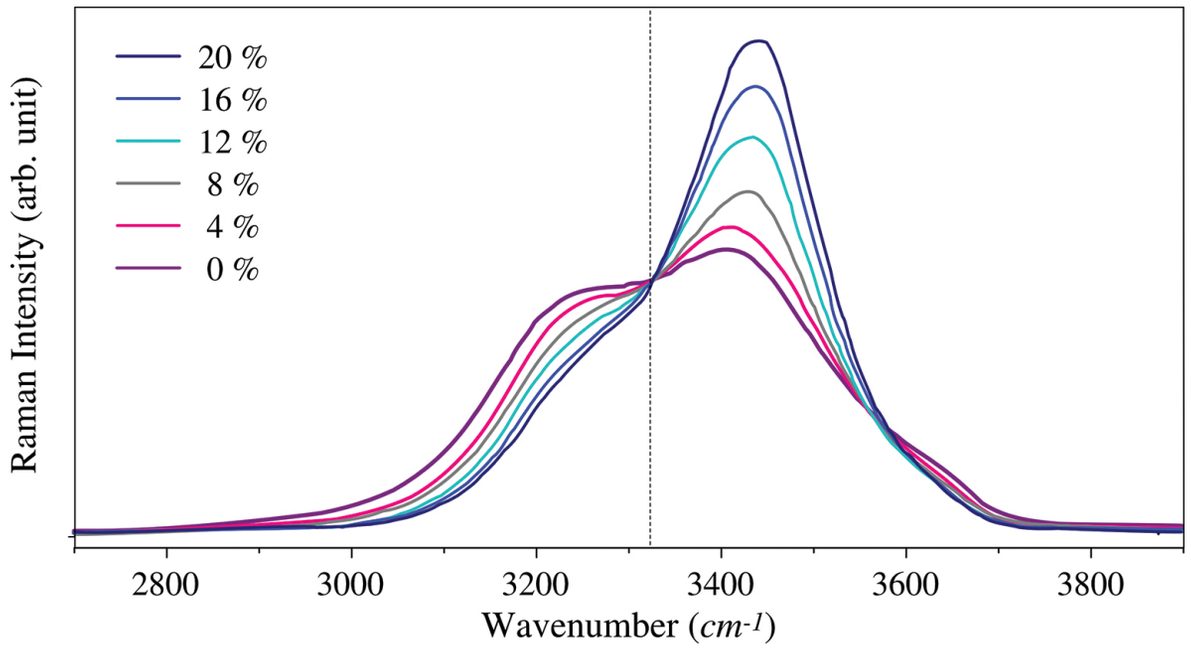


**Figure 11.** O—H stretching region of Raman spectra of NaCl aqueous solutions in a weight percent up to 20%.

**Figure 11** shows the influence of NaCl concentration dissolved in water on its Raman spectrum. Two main effects can be underlined: NaCl affects both the O—H symmetric and O—H asymmetric stretch. The concentration increase enhances the morphological changes of the O—H

stretching band, diminishing the O—H symmetric and increasing the O—H asymmetric stretching vibrations [51], leading to a spectrum shift towards higher wavenumbers. This can be considered as a direct result of the dissolution of NaCl in water, which provokes the decrease of the number of hydrogen bonds in the intermolecular structure [50, 52, 53].

It is then possible to use the ratio of the asymmetric and symmetric O—H stretching vibrations as a spectral marker for the elaboration of the calibration curve [54]. The O—H stretching band was then divided into two parts, 3325–3650 $cm^{-1}$ as representative of the O—H asymmetric stretching vibrations, and 3000–3325 $cm^{-1}$ as representative of the O—H symmetric stretching vibrations.

After an elaboration of a calibration curve, a set of blind tests should be performed in order to verify the uncertainty of this indirect way of concentration determination. The plot presenting the calculated concentration via the experimental $S_D$ versus the theoretically calculated concentration is presented in **Figure 12**.

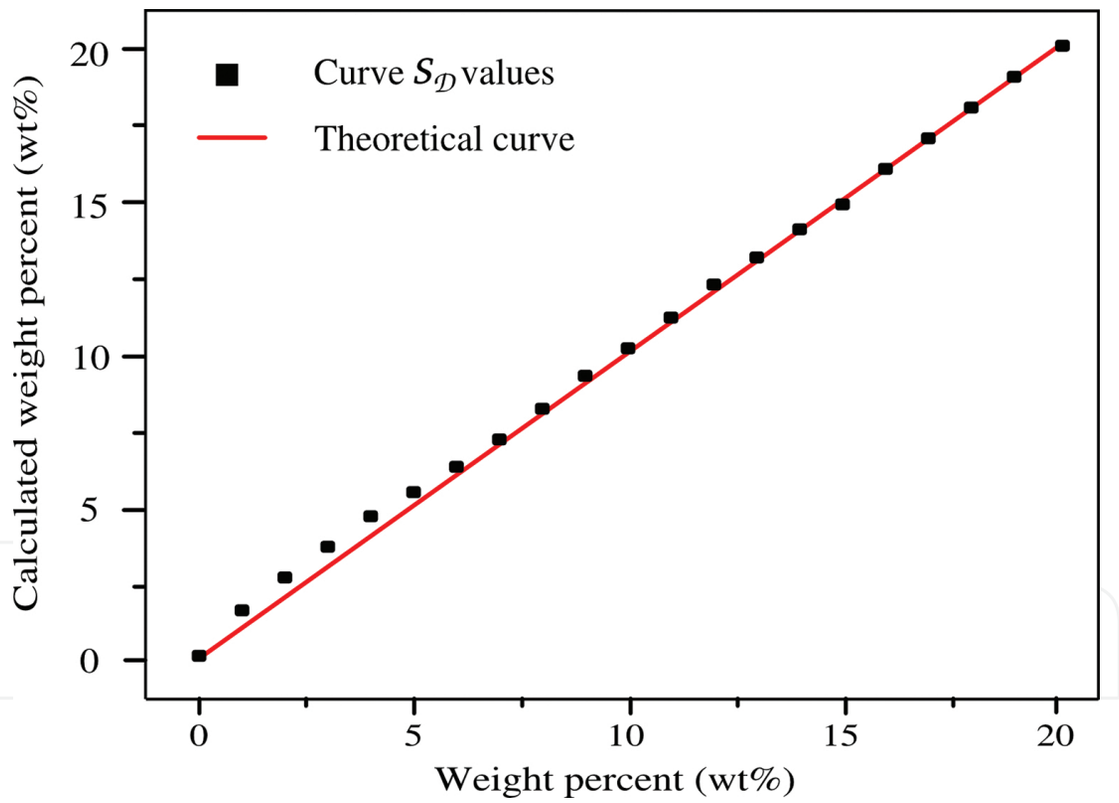


**Figure 12.** Comparison of calculated weight percent (represented by the experimental points in black) and weight percent (represented by the curve in red).

As shown in the **Figure 12**, even an indirect way of concentration determination can offer good precision, especially for more concentrated solutions; For this specific case, the standard deviation is of 0.25% for weight percentages over 7 and of 0.75% for weight percentages up to 5%.

http://dx.doi.org/10.5772/64550

To sum up, this approach can also be applied to all salts that dissolve into monoatomic ions, since in their dissolved form they interact with water, and these interactions are detectable and quantifiable by the means of the Raman spectra of water. Hence, similar studies even in applications other than the winter maintenance domain were also conducted, for example on the effect of different alkali halide on the water structure [50, 51]. These studies showed that the influence of dissolved salts on water structure depends on the size and the charge of the ions, as well as the strength they form with the O—H complex.

It is also possible to analyze the O—H stretching band for the quantification of dissolved salts in solutions where several salts are present. For instance, quantification of NaCl with a 0.14 wt % error was realized in a solution of NaCl and NaF at 2.8 wt% [55].

*4.1.2. Phase diagram elaboration*

The method described in Section 3.3 can also be applied to aqueous solutions where the main morphological change appearing with the phase change concerns the O—H stretching band. It is then possible to apply exactly the same spectral marker as for water for the detection of the phase transition, that is to say a ratio of integrated intensities of the asymmetric and the symmetric part of the O—H band.

The analysis of a set of aqueous solutions at different concentrations in a large range of temperature can therefore permit the construction of the phase diagram which has a capital importance in the winter maintenance domain. With a large temperature range, it is possible to detect the different phase transitions. Indeed, in mixtures such as aqueous solutions, upon cooling down, each component will solidify at a different temperature. The first phase transition will then be a transition from a liquid to a mixture of liquid and solid phases. For binary systems, where only two components are present, the second phase transition will then transform the solid-liquid mixture into an entirely solid. For illustration purpose, the NaCl-$H_2O$ phase diagram is presented **Figure 13**.

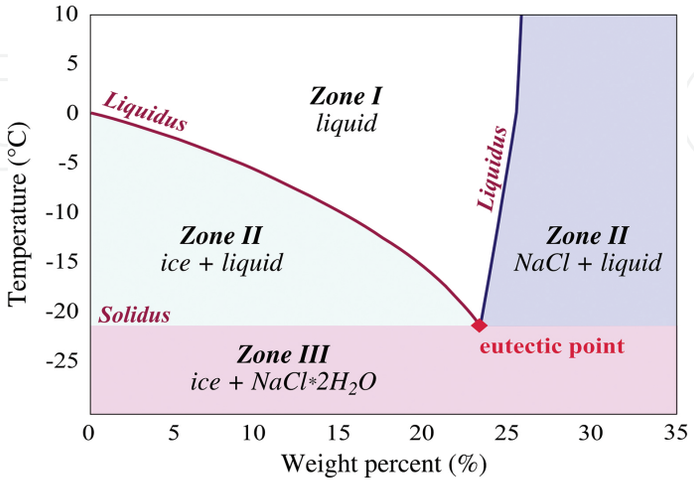


**Figure 13.** Phase diagram of the NaCl-$H_2O$ binary system.

Upon cooling down a mixture of NaCl and water, the ice will be formed below a certain temperature of the so-called *liquidus* curve, this temperature being dependent on the brine concentration. During a certain temperature range, the mixture will be then composed of ice and liquid brine (Zone II). Upon further cooling down, at some point the entire mixture will solidify into ice and a hydrated form of NaCl (Zone III). This second phase transition will occur at temperatures below the *solidus* line, which is located at the eutectic temperature. The concentration of the eutectic point permits to determine the precise hydrated form of salt.

Such a phase diagram can be built experimentally by applying the spectroscopic method described before to any aqueous solutions [56].

### 4.2. Application to water pollution

Another application example could be the detection of water pollutants where there is an increasing need for a technique that could permit an *on-site* detection of the pollution sources. Many pollutant families are identified as being potentially very harmful for the environment and thus it is important to survey. As an example, we can cite the pollutants coming from the agricultural activities, such as the fertilizers, nitrates, or phosphates, or some drugs, such as hormones, which can have particularly important impacts on the environmental media.

In that objective, many studies have investigated the possibility to use optical methods, and more specifically RS for the detection of pollutants in water media [57, 58]. The method described earlier in this chapter, based on the calculation of ratios of pollutant-specific peak and water peak, can then also be applied to water pollutants [59, 60].

## Author details

Ivana Durickovic

Address all correspondence to: ivana.durickovic@cerema.fr

Centre for Studies and Expertise on Risks, Environment, Mobility, and Urban and Country Planning Territorial Division for Eastern Regions – Laboratory of Nancy, Tomblaine, France

## References

[1] McMillan P. Vibrational spectroscopy in the mineral sciences. In: Kieffer SW, Navrotsky A, editors. Microscopic to Macroscopic: Atomic Environments to Mineral Thermodynamics. Volume 14. Washington: Mineralogical Society of America; 1985, p. 9-64.

[2] Bhadekar R, Pote S, Tale V, Nirichan B. Mint: Developments in analytical methods for detection of pesticides in environmental samples. American Journal of Analytical Chemistry. 2011;2:1-15. DOI: 10.4236/ajac.2011.228118.

[3] Storey MV, van der Gaag B, Burns BP. Mint: Advances in on-line drinking water quality monitoring and early warning systems. Water Research. 2011;45:741-747.

[4] AU: Please provide location details for Refs. [4, 5, 38].Colthup NB, Daly LH, Wiberly SE. Introduction to Infrared and Raman Spectroscopy. 3rd ed., Academic Press; 1990.

[5] Larkin PJ. IR and Raman Spectroscopy: Principles and Spectral Interpretation. Elsevier; 2011. 535 p.

[6] AU: Please provide the journal title in English and also provide complete details for Ref. [6].Colomban P. Raman imaging of materials and heterogeneous devises. In: Techniques de l'Ingénieur. 2002. RE-5, p. 13

[7] Baia M, Astilean S, Illiescu T. Raman and SERS Investigations of Pharmaceuticals. Berlin: Springer; 2008.

[8] Claverie R, Fontana MD, Durickovic I, Bourson P, Marchetti M, Chassot JM. Mint: Optical sensor for characterizing the phase transition in salted solutions. Sensors. 2010;10:3815-3823. DOI: 10.3390/s100403815.

[9] Lewis IR, Edwards HGM, editors. Handbook of Raman Spectroscopy: From the Research Laboratory to the Process Line. New York: Marcel Dekker; 2001.

[10] AU: Please provide the journal title in English for Ref. [10].Barbillat J. Spectrométrie Raman. Techniques de l'Ingénieur. 1999;9:2865-1-2865-31.

[11] Walrafen GE, Blatz LA. Mint: Weak Raman bands for water. The Journal of Chemical Physics. 1973;59:2646-2650. DOI: 10.1063/1.1680382.

[12] Auer BM, Skinner JL. Mint: IR and Raman spectra of liquid water: Theory and interpretation. The Journal of Chemical Physics. 2008;128:224511-1224511-12. DOI: 10.1063/1.2925258.

[13] Carey MD, Korenowski GM. Mint: Measurement of the Raman spectrum of liquid water. Journal of Chemical Physics. 1998;108:2669-2675. DOI: 10.1063/1.475659.

[14] Eisenberg D, Kauzmann W. The water molecule. In: Pauling L. The Structure and Properties of Water. London: Oxford University Press; 1969. p. 1-34.

[15] Pimentel GC, McClellan AL. The Hydrogen Bond. San Francisco: Freeman; 1960

[16] Shriver P., Atkins W. Inorganic Chemistry. 3rd ed. Oxford: Oxford University press; 1999. 706 p.

[17] Max JJ, Chapados C. Mint: Isotope effects in liquid water by infrared spectroscopy. III. $H_2O$ and $D_2O$ spectra from 6000 to 0 $cm^{-1}$. Journal of Chemical Physics. 2009;131:4626. DOI: 10.1063/1.1448286.

[18] Sun G. Mint: The Raman OH stretching bands of liquid water. Vibrational Spectroscopy. 2009;51:213-217. DOI: 10.1016/j.vibspec.2009.05.002.

[19] Pershin SM. Mint: Structure of the Raman band of the OH stretching vibrations of water and its evolution in a field of second harmonic pulses of a Nd:YAG laser. Molecular Spectroscopy. 2004;96:811-815. DOI: 10.1134/1.1771411.

[20] Bunkin AF, Pershin SM, Rashkovich LN. Mint: Changes in the Raman spectrum of OH stretching vibrations of water in an ultrasonic cavitation field. Molecular Spectroscopy. 2004;96:512-514. DOI: 10.1134/1.1719137.

[21] Kargovsky AV. Mint: On temperature dependence of the valence band in the Raman spectrum of liquid water. Laser Physics Letters. 2006;3:567-572. DOI: 10.1002/lapl.200610063.

[22] Laubereau A., Laenen R. Ultrafast coherent Raman and infrared spectroscopy of liquid systems. In: Fayer MD, editor. Ultrafast Infrared and Raman Spectroscopy. New York: Marcel Dekker; 2001. p. 1-80.

[23] Skinner JL, Auer BM, Lin YS. Mint: Vibrational line shapes, spectral diffusion, and hydrogen bonding in liquid water. Advances in Chemical Physics. 2009;142:59-103. DOI: 10.1002/9780470475935.ch2

[24] Risovic D, Furic K. Mint: Comparison of Raman spectroscopic methods for the determination of supercooled and liquid water temperature. Journal of Raman Spectroscopy. 2005;36:771-776. DOI: 10.1002/jrs.1359

[25] Walrafen G. Mint: Raman spectral studies of the effects of temperature on water structure. Journal of Chemical Physics. 1967;47:114-126. DOI: 10.1063/1.1711834.

[26] Scherer JR, Go MK, Kint S. Mint: Raman spectra and structure of water from −10 to 90 deg. The Journal of Physical Chemistry. 1974;78:1304-1313. DOI: 10.1021/j100606a013.

[27] Chumaevskii NA, Rodnikova MN. Mint: Some peculiarities of liquid water structure. Journal of Molecular Structure. 2003;106:167-177. DOI: 10.1016/S0167-7322(03)00105-3.

[28] Durickovic I. Study of the residual salinity by Raman spectroscopy [thesis]. Metz: University of Paul Verlaine – Metz; 2008.

[29] Sun Q. Mint: The single donator-single acceptor hydrogen bonding structure in water probed by Raman spectroscopy. Journal of Chemical Physics. 2010;132:054507. DOI: 10.1063/1.3308496.

[30] Walrafen GE. Raman and infrared spectral investigations of water structure. In: Franks F., editor. The Physics and Physical Chemistry of Water. New York: Springer; 1972. p. 151-214. DOI: 10.1007/978-1-4684-8334-5_5.

[31] Walrafen GE. Mint: Effects of equilibrium H-bond distance and angle changes on Raman intensities from water. Journal of Chemical Physics. 2004;120:4868-4876. DOI: 10.1063/1.1640668.

[32] Rey R, Moller KB, Hynes JT. Mint: Hydrogen bond dynamics in water and ultrafast infrared spectroscopy. Journal of Physical Chemistry A. 2002;106:11993-11996. DOI: 10.1021/jp026419o.

[33] Schmidt DA, Miki K. Mint: Structural correlations in liquid water: A new interpretation of IR spectroscopy. Journal of Physical Chemistry A. 2007;111:10119-10122. DOI: 10.1021/jp074737n.

[34] Kitadai N, Sawai T, Tonoue R, Nakashima S, Katsura M, Fukushi K. Mint: Effects of ions on the OH stretching band of water as revealed by ATR-IR spectroscopy. Journal of Solution Chemistry. 2014;43:1055-1077. DOI: 10.1007/s10953-014-0193-0.

[35] Beccucci M, Cavalieri S, Eramo R, Fini L, Materazzi M. Mint: Accuracy of remote sensing of water temperature by Raman spectroscopy. Applied Optics. 1999;38:928-931. DOI: 10.1364/AO.38.000928.

[36] Praprotnik M, Janezic D, Mavri J. Mint: Temperature dependence of water vibrational spectrum: A molecular dynamics simulation study. Journal of Physical Chemistry A. 2004;108:11056-11062. DOI: 10.1021/jp046158d

[37] Durickovic I, Claverie R, Bourson P, Marchetti M, Chassot JM, Fontana MD. Mint: Water-ice phase transition probed by Raman spectroscopy. Journal of Raman Spectroscopy. 2011;42:1408-1412. DOI: 10.1002/jrs.2841

[38] U.S. Department of Transportation. Manual of Practice for an Effective Anti-icing Program: A Guide for Highway Winter Maintenance Personnel. Federal Highway Administration; 1996.

[39] Switzenbaum MS, Veltman S, Schoenberg T, Durand CM. Best Management Practices for Airport Deicing Stormwater. Amherst: Department of Civil and Environmental Engineering, University of Massachusetts; 1999. 57 p.

[40] National Cooperative Highway Research Program. Snow and Ice Control: Guidelines for Materials and Methods. Washington: Transportation Research Board; 2004.

[41] Airport Cooperative Research Program. Impact of Airport Pavement Deicing Products on Aircraft and Airfield Infrastructure. Washington: Transportation Research Board; 2008.

[42] Frost RL, Kloprogge JT. Mint: Raman spectroscopy of the acetates of sodium, potassium and magnesium at liquid nitrogen temperature. Journal of Molecular Structure. 2000;526:131-141. DOI: 10.1016/S0022-2860(00)00460-9.

[43] Yang RD, Tripathy S, Li Y, Sue HJ. Mint: Photoluminescence and micro-Raman scattering in ZnO nanoparticles: The influence of acetate adsorption. Chemical Physics Letters. 2005;411:150-154. DOI: 10.1016/j.cplett.2005.05.125

[44] Tse WS, Chiang PY, Lin SJ. Mint: A Raman spectral study of the phase transitions in crystalline potassium acetate. Chinese Journal of Physics. 1986;24:63-68.

[45] Musumeci AW, Frost RL, Waclawik ER. Mint: A spectroscopic study of the mineral paceite (calcium acetate). Spectrochimica Acta Part A: Molecular and Biomolecular Spectroscopy. 2007;67:649-661. DOI: 10.1016/j.saa.2006.07.045.

[46] AU: Please provide complete details for Ref. [46].Poulston S, Holroyd RP, Bowker M, Parker SF, Mitchell PCH. Mint: Molecular spectroscopy of formates on copper surfaces. Scientific Highlights.

[47] Robinet L, Eremin K, Cobo des Arco B, Gibson LT. Mint: A Raman spectroscopic study of pollution-induced glass deterioration. Journal of Raman Spectroscopy. 2004;35:662-670. DOI: 10.1002/jrs.1133.

[48] Mitchell PCH, Holroyd RP, Poulston S, Bowker M, Parker SF. Mint: Inelastic neutron scattering of model compounds for surface formates. Potassium copper formate and formic acid. Journal of Chemical Society, Faraday Transitions. 1997;93:3569-3575.

[49] Bakker RJ. Mint: Raman spectra of fluid and crystal mixtures in the systems H2O, H2O-NaCl and H2O-MgCl2 at low temperatures: Applications to fluid-inclusion research. The Canadian Mineralogist. 2004;45:1283-1314.

[50] Terpstra P, Combes D, Zwick A. Mint: Effect of salts on dynamics of water: A Raman spectroscopy study. Journal of Chemical Physics. 1990;92:65-70.

[51] Schultz JW, Hornig DF. The effect of dissolved alkali halides on the Raman spectrum of water. Journal of Physical Chemistry. 1961;65:2131-2138. DOI: 10.1021/j100829a005.

[52] Hibben JH. Mint: The Raman spectra of water, aqueous solutions and ice. Journal of Chemical Physics. 1937;5:166-172. DOI: 10.1063/1.1750001.

[53] Rull F. Mint: Structural investigation of water and aqueous solutions by Raman spectroscopy. Pure Applied Chemistry. 2002;74:1859-1870. DOI: 10.1351/pac200274101859.

[54] Durickovic I, Marchetti M, Claverie R, Bourson P, Chassot JM, Fontana MD. Mint: Experimental study of NaCl aqueous solutions by Raman spectroscopy: Towards a new optical sensor. Applied Spectroscopy. 2010;64:853-857.

[55] Burikov SA, Dolenko TA, Fadeev VV, Sugonyaev AV. Mint: Identification of inorganic salts and determination of their concentrations in aqueous solutions based on the valence Raman band of water using artificial neural networks. Applied Problems. 2007;17:554-559. DOI: 10.1134/S1054661807040141.

[56] Durickovic I, Thiebaud L, Bourson P, Kauffmann T, Marchetti M. Mint: Spectroscopic characterization of urea aqueous solutions: Experimental phase diagram of the urea-water binary system. Applied Spectroscopy. 2013;67:1205-1209. DOI: 10.1366/12-06870.

[57] Li Z, Deen MJ, Kumar S, Selvaganapathy PR. Mint: Raman spectroscopy for in-line water quality monitoring – instrumentation and potential. Sensors. 2014;14:17275-17303. DOI: 10.3390/s140917275.

[58] Braunlich G, Gamer G, Petty MS. Mint: Detection of pollutants in water by Raman spectroscopy. Water Research. 1973;7:1643-1647. DOI: 10.1016/0043-1354(73)90133-4.

[59] Ben Mabrouk K, Kauffmann TH, Fontana MD. Mint: Abilities of Raman sensor to probe pollutants in water. Journal of Physics: Conference Series. 2013;450:012014. DOI: 10.1088/1742-6596/450/1/012014.

[60] Durickovic I, Marchetti M. Mint: Raman spectroscopy as a polyvalent alternative for water pollution detection. IET Science, Measurement and Technology. 2014;8:122-128. DOI: 10.1049/iet-smt.2013.0143.

IntechOpen